

COVID-19 Ocular Prophylaxis: The Potential Role of Ozonated-Oils in Liposome Eyedrop Gel

Stanislao Rizzo^{1-3,*}, Maria Cristina Savastano^{1,2,*}, Daria Bortolotti⁴, Alfonso Savastano^{1,2}, Gloria Gambini^{1,2}, Francesca Caccuri⁵, Valentina Gentili^{4,‡}, and Roberta Rizzo^{4,‡}

¹ Unit of Ophthalmology, "Fondazione Policlinico A Gemelli IRCCS," Rome, Italy

² "Università Cattolica Sacro Cuore," Rome, Italy

³ Consiglio Nazionale delle Ricerche (CNR), Istituto di Neuroscienze, Pisa, Italy

⁴ University of Ferrara, Department of Chemical, Pharmaceutical and Agricultural Sciences, Ferrara, Italy

⁵ Department of Microbiology and Virology, "Spedali Civili," Brescia, Italy

Correspondence: Daria Bortolotti, University of Ferrara - Department of Chemical, Pharmaceutical and Agricultural Sciences, Via Luigi Borsari, 46, 44121 Ferrara -Italy. e-mail: daria.bortolotti@unife.it

Received: April 9, 2021

Accepted: June 21, 2021

Published: August 5, 2021

Keywords: ozonated-oil in liposome eyedrop gel; innovative biotechnologies; personalized medicine; prophylaxis agent; SARS-CoV-2

Citation: Rizzo S, Savastano MC, Bortolotti D, Savastano A, Gambini G, Caccuri F, Gentili V, Rizzo R. COVID-19 ocular prophylaxis: The potential role of ozonated-oils in liposome eyedrop gel. *Transl Vis Sci Technol.* 2021;10(9):7. <https://doi.org/10.1167/tvst.10.9.7>

Purpose: To assess whether ozonated-oil in liposome eyedrop gel (OED) could be used to prevent the severe acute respiratory syndrome-coronavirus 2 (SARS-CoV-2) infection in an in vitro infection model.

Methods: First, we tested the efficacy of OED on in vitro cell regeneration and dry eye resolution in human corneal epithelial cells (hCE-2). Second, we assessed the in vitro anti-SARS-CoV-2 infection efficacy of OED using Vero E6 cells. Tissues were examined to assess different parameters: morphology, histology, and mRNA expression at 24 hours after treatment.

Results: OED could restore 50% of the scratch in the monolayer of hCE-2 cells in vitro compared with the 25% obtained with phosphate-buffered saline solution (PBS). At 24 hours after treatment with OED, the number of microvilli and the mucin network were restored, as observed using scanning electron microscopy. In Vero E6 cells infected with a primary SARS-CoV-2 strain and treated with OED two times/day, viral replication was found to be inhibited, with a 70-fold reduction observed at 72 hours after infection compared with that under the untreated and PBS-treated conditions.

Conclusions: SARS-CoV-2 transmission through the ocular surface should not be ignored. Although the prevalence of coronavirus disease 2019 conjunctivitis infection is low, the need for a barrier to prevent possible viral infection is warranted. OED treatment may prevent the risk of SARS-CoV-2 infection after 72 hours of twice-daily applications.

Translational Relevance: Dry eye condition might be a risk factor for SARS-CoV-2 infection and OED treatment may have a preventive role.

Introduction

The first report of ocular manifestation among COVID-19 patients was provided by a member of the National Expert Panel on Pneumonia, who was infected during his inspection in Wuhan, despite wearing an N95 mask.¹ This expert did not wear an eye protection or face shield, and several days before developing pneumonia, he reported redness of his eyes, which led to the suggestion that unprotected exposure

of the eyes might have allowed the virus to infect the body.¹ Isolated case studies have described the virus persistence in the ocular surface past the initial infection phase. Chen et al.² indicated the development of bilateral acute follicular conjunctivitis at day 13 of illness in a 30-year-old COVID-19 patient, with SARS-CoV-2 RNA being present in the conjunctival specimens between 9 and 18 days of disease. Prolonged presence of viral RNA has also been described in a clinical case report of a Chinese COVID-19-positive patient who traveled from China to Italy and presented

with bilateral conjunctivitis at day 1 of hospitalization. Viral RNA was detected by reverse transcriptase polymerase chain reaction (RT-PCR) on the conjunctival swab samples from day 3 to day 21 at lower Ct values than nasal swabs. Although no viral RNA was detected between days 22 and 26 in both nasal and conjunctival swabs, low expression was detected in conjunctival swabs at day 27, which indicates a sustained infection, also corroborated by the successful viral inoculation in Vero E6 cells.³ To ascertain the impacts of COVID-19 on the ocular surface, a prospective observational study assessed 38 confirmed COVID-19 patients and 31 healthy controls.⁴ Although no significant differences were observed regarding age and gender between the two groups, conjunctival impression cytology revealed decreased density and enlargement of goblet cells, squamous changes, and increased presence of neutrophils in the COVID-19 patients. Together these data demonstrate that SARS-CoV-2 infection of the ocular surface is observed at low frequency.⁵ Possibly corneal and conjunctival epithelial cells are protected by the tear film and the fast drainage (approximately every five minutes) that might provide a barrier for infection of the underlying epithelia. It has been postulated that the tear film, particularly the superficial lipid layer, may act as a barrier to prevent SARS-CoV-2 binding to the corneal/conjunctival epithelia entry receptors. Furthermore, the tear flow may provide an “ocular surface wash-out” effect, preventing prolonged persistence of virus on the ocular surface. Nonetheless, if the virus makes its way to the ocular surface epithelium, through the tear film, tear flow and drainage may facilitate a second route of infection binding to receptors in and beyond the nasolacrimal system.⁶

Recent studies have focused on viral interactions between viral glycoproteins and human host receptors to better understand the mechanism of virus entry into cells.⁷ One possible interference of a virus' access to cells is ozone (O₃).⁸ O₃ gas is a molecule consisting of three oxygen atoms in a dynamically unstable structure because of the presence of mesomeric states.⁹

The potential effect of ozone is related to the control of inflammation, stimulation of immunity, and antiviral activity, suggesting a new methodology for immune therapy.¹⁰ O₃ therapy has been recognized as one of the best antimicrobial agents,^{11,12} possibly associated to the transient, and moderate, oxidative stress that O₃ induces. O₃ can cause this mild oxidative stress because of its ability to dissolve in the aqueous component of the ocular surface and to react with polyunsaturated fatty acids and water, creating hydrogen peroxide. Moderate oxidative stress caused by O₃ increases the activation of the transcriptional factor

mediating nuclear factor-erythroid 2-related factor 2 (Nrf2).¹³ Nrf2's domain is responsible for activating the transcription of antioxidant response elements. The induction of antioxidant response elements transcription raises antioxidant enzymes activation in response to the transient oxidative stress of O₃. The antioxidants created include, but are not limited to, superoxide dismutase, glutathione peroxidase, glutathione S-transferase, catalase, heme oxygenase-1, NADPH quinone-oxidoreductase (NQO-1), heat shock proteins (HSP), and phase II enzymes of drug metabolism. Many of these enzymes act as free radical scavengers clinically relevant to a wide variety of diseases.¹³

O₃ is used medically to disinfect and treat infectious diseases and inactivate bacteria, viruses, fungi, yeast, and protozoa. The efficacy of O₃ toward enveloped viruses might be related to its ability to damage and enclose the viral capsid, thereby upsetting the viral replication with peroxidation. Medications of a gaseous nature are somewhat unusual, and ozone in the form of O₃ gas is extremely reactive and is not always suitable as a topical treatment. For this reason, special applications have been developed. Interestingly, despite its instability, the ozone molecule can be stabilized for topical use by creating ozonide through a reaction between ozone and the double bonds of a monounsaturated fatty acid, such as oleic acid,¹⁴ and the derived compounds are known as “ozonated oils” (Fig. 1).

Ozonated oils have the same properties and activities as gaseous ozone and are well tolerated by biological tissues. Furthermore, their biological activities are related to oxygenated compounds.^{15,16} In particular, ozonated oils are new products for the treatment of ocular pain and inflammation that occur during events, such as external ocular infections and inflammation, because of the related risk of blindness.

Ozonated oil can eliminate pathogens by direct oxidation mediated by hydrogen peroxide, lipoperoxidation, and selective cytotoxicity on fast-dividing cells. These actions occur through bacterial lysis and cell death, negative regulation of mitochondrial activity in bacteria, and disturbance of viral lithic enzymes in superimposable manners as compared to the action of phagocytic cells of the immune system.¹⁷

Ozone allows “physiological” wound healing, which minimizes the risk of keloidal scarring and haze in the cornea. According to Marchegiani et al., liposomal ozone-dispersion is as effective as povidone iodine for reducing bacterial load on the ocular surface.¹⁸ As a result, this nanoformulation has recently been developed for ophthalmic use, and its potential antiseptic prophylactic effects against SARS-CoV-2 have been described by Mazzotta et al.¹⁹

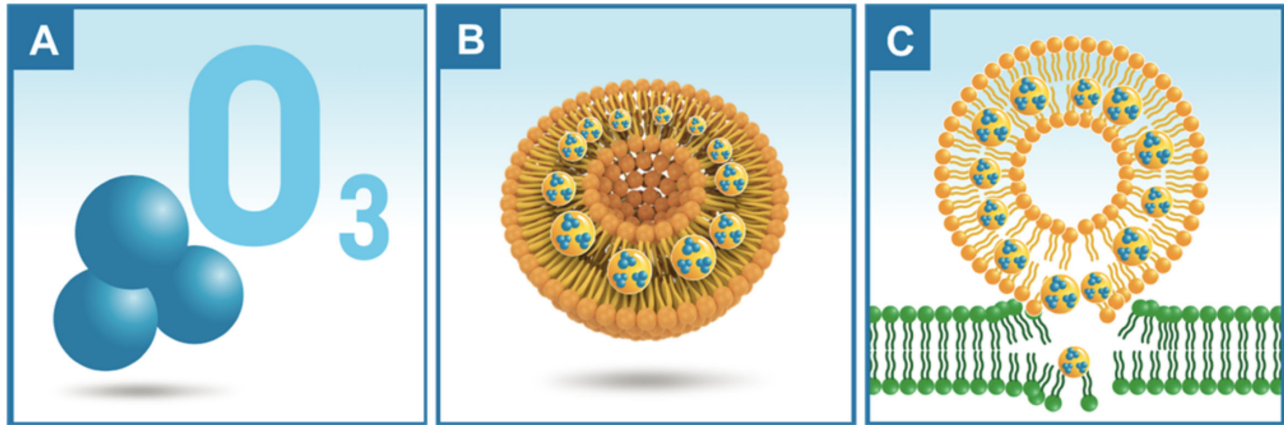


Figure 1. (A) Three oxygen atoms cause the O_3 molecule to be highly unstable. (B) The ozone molecule can only be stabilized via enveloping in micellar lipid solution called “ozonated oil.” (C) The lipid portion of the micelle binds to the lipid portion of the virus membrane, which releases O_3 when the viral capsid is disrupted.

Because the integrity of cells and the penetration of SARS-CoV-2 are closely interconnected, we decided to evaluate the in vitro efficacy of ozonated-oil in liposome eyedrop gel (OED) on human corneal epithelial cells (hCE-2) infected by SARS-CoV-2. Concerning the ocular surface, the presence of small damage, such as in dry eye disease (DED), induces high vulnerability to microorganism penetration and infection.²⁰ In this condition, the necessity to prevent microorganisms infection is of extreme importance. The restoring the ocular surface may further prevent the entry of pathogens into cells.

On the basis of such knowledge, we assessed also the possible prophylactic effect of OED in controlling SARS-CoV-2 infection in pathological conditions as DED. This goal includes the evaluation of the efficacy of OED in repairing and regenerating conjunctival microvilli defects, such as in DED.

Methods

The study was approved by the Catholic University/Fondazione Policlinico A. Gemelli IRCCS Institutional Ethics Committee (Protocol number: 0013008/20. ID: 3045). All authors reviewed the manuscript and declare the accuracy and completeness of the data and adherence to the study protocol.

The study was divided into two phases. In the first phase, we determined the in vitro efficacy of OED on hCE-2 with DED. In the second phase, we assessed the in vitro efficacy of OED in Vero E6 cells for the COVID-19 infection. All experiments were performed in triplicates.

Phase One: In Vitro Efficacy of OED on hCE-2 Cells

Scratch Test

The scratch test is generally applied to cells in vitro to assess the regeneration capability of damaged cells after the use of a particular substance (in our case). The hCE-2 cell line (number CRL-11135; ATCC, Manassas, VA, USA) was cultured in keratinocyte serum-free medium (number 17005-042; Gibco, Thermo Fisher Scientific, Waltham, MA, USA) supplemented with 0.05 mg/mL bovine pituitary extract (Gibco), 5 ng/mL epidermal growth factor, 500 ng/mL hydrocortisone, and 0.005 mg/mL insulin (Gibco). The cells were cultured in a culture-insert two-well (Ibidi USA, Fitchburg, WI, USA) to obtain a scratch. After 24 hours, the inserts were removed, and 100 to 500 μ L of OED (Ozodrop-GEL; FBVision, San Benedetto del Tronto, Italy) were added to the test sample. Images of the wounded areas were captured before the addition of the OED and after 24 hours of treatment. The control group received 1x phosphate-buffered saline solution (PBS; Gibco). The wound area was assessed at 0 and 24 hours using Adobe Photoshop Elements 2020. The treated samples were compared to the controls.

Experimentally Induced in Vitro Dry Eye in Human Corneal Tissues

Corneal tissues were obtained from “Eye Biobank: Fondazione Banca degli Occhi del Veneto.” The human corneal tissue contains the metabolic, functional, and anatomical features of the living organ, and therefore there is no need to provide evidence of its similarity to natural cornea. Thirty minutes before measurements, all corneal tissues were raised to a temperature

of 32°C, corresponding to the corneal surface temperature observed in humans.²¹ Corneal tissues were placed under controlled environmental conditions to mimic dryness (<40% relative humidity, 40° ± 5 °C temperature, and 5% CO₂) for 24 hours.

The corneal tissues were then treated with 100 µL/day of OED. A similar culture was treated with two 100 µL/day of PBS to serve as the control. Tissues were investigated to assess different parameters: morphology, histology, and mRNA expression of selected genes at 24 hours after treatment.

Evaluation of Microvilli and Mucins Using Scanning Electron Microscopy

Corneal tissues were fixed in 2.5% glutaraldehyde in 0.1 M phosphate buffer for two hours at 4°C. After the samples were washed three times for five minutes with 0.1 M phosphate buffer, they were placed in 1% OsO₄ in 0.1 M phosphate buffer. Samples were dehydrated using a graded series of ethanol and a graded series of hexamethyldisilane. Specimens were mounted on aluminum stubs with silver-conducting paint, coated with the gold sputter coater, Quorum Q 150R S, and observed under the scanning electron microscope, Zeiss Evo 40 (Zeiss, Oberkochen, Germany).

Histological Analysis

At the end of OED treatment, corneal tissues were fixed in 10% formalin solution (HT501128). After embedding in paraffin, vertical sections (4 µm thick) were cut with a microtome and stained with hematoxylin and eosin. Histological samples were analyzed under a light microscope, and the overall morphology of the epithelium and its modifications were compared to those of the control samples.

Transcriptional Study of mRNA (qRT-PCR)

mRNA was extracted from the corneal tissues using the RNeasy Mini Kit (Qiagen, Hilden, Germany), according to the manufacturer's protocol. Subsequently, the cDNAs were synthesized using the SuperScript kit (ThermoFisher, St. Louis, MO, USA). Real time polymerase chain reaction was performed in triplicate in a final reaction volume of 25 µL using the ABI PRISM 7500 Real Time PCR System (Applied Biosystems, Foster City, CA, USA) with TaqMan assay (Ambion-Applied Biosystems, Austin, TX, USA). The cDNA was amplified using TaqMan Universal PCR Master Mix and TaqMan gene expression assay provided as a 20 × Assay mix (Human MMP9: TaqMan probe MMP9 Hs00234579_m1; Human IL-8: TaqMan probe IL-8 Hs00174103_m1; Human GAPDH as the calibrator gene: Taqman probe GAPDH Hs99999905_m1). The PCR conditions were

95°C for 10 minutes (AmpliTaq Gold DNA polymerase activation) followed by 40 amplification cycles (95°C for 15 seconds, then 60°C for one minute). The relative gene expression was calculated using the 2^(-Delta C[T]) method.

Phase 2: In Vitro Anti-SARS-CoV-2 Infection Efficacy of OED in Vero E6 Cells

Cell Viability Assay

At different time points after treatment with different concentrations of OED (100-500 µL), cell viability was examined by Trypan blue dye exclusion (Roche Diagnostics Corporation, Basel, Switzerland), as previously described.^{22,23}

SARS-CoV-2 Infection

Vero E6 cells (ATCC CRL-1586) were grown as described previously.^{15,16} SARS-CoV-2 was isolated from a nasopharyngeal swab retrieved from a patient with COVID-19 (Caucasian man of Italian origin, genome sequences available at GenBank (SARS-CoV-2-UNIBS-AP66: ERR4145453).²⁴ This SARS-CoV-2 isolate clustered in the B1 clade, which includes most of the Italian sequences, together with sequences derived from other European countries and the United States. The identity of the strain was verified in Vero E6 cells using real-time PCR and metagenomic sequencing, from which the reads were mapped to nCoV-2019 (genomic data are available at EBI under study accession no. PRJEB38101). We propagated the clinical isolate in Vero E6 cells and determined the viral titer using a standard plaque assay. The infection experiments were carried out in a biosafety level-3 (BLS-3) laboratory at multiplicity of infections (MOIs) of 0.05 and 1.0.²² Vero E6 cells were seeded at a density of 5 × 10⁴ cells/well in a 24-well plate and infected for one hour with the SARS-CoV-2 isolate at an MOI of 0.05. The infection was carried out in Dulbecco's modified Eagle's medium (Gibco) without fetal bovine serum (FBS). After virus removal and washing with warm PBS (Gibco; USA), the cells were cultured in medium containing 2% fetal bovine serum (Gibco) in the presence or absence of 100 µL of OED or PBS as the control. At 24, 48, and 72 hours after infection, both the cells and supernatants were collected for further viral genome quantification analysis.

Viral RNA Extraction and Quantitative Reverse Transcription-PCR

RNA was extracted from clarified cell culture supernatants (16,000g for 10 minutes) and infected

cells using a QIAamp Viral RNA Mini Kit and RNeasy Plus mini kit (Qiagen), respectively, according to the manufacturer's instructions. RNA was eluted in 30 μ L of RNase-free water and stored at -80°C until use. Quantitative reverse transcription PCR (qRT-PCR) was carried out following previously described procedures with minor modifications.¹⁶ Briefly, reverse transcription and amplification of the S gene were performed using the one-step QuantiFast SYBR Green RT-PCR mix (Qiagen) and the following cycling profile: 50°C for 10 minutes, 95°C for five minutes; 95°C for 10 seconds, 60°C for 30 seconds (40 cycles) (primers: RBD-qF1: 5'-CAATGGTTTAACAGGCACAGG-3' and RBD-qR1: 5'-CTCAAGTGTCTGTGGATCACG-3'). A standard curve was generated by determining the copy numbers derived from serial dilutions (10^3 – 10^9 copies) of the pGEM T-easy vector (Promega, Madison, WI, USA) containing the receptor-binding domain of the S gene (primers: RBD-F: 5'-GCTGGATCCCCTAATATTACAAACTTGTGCC-3'; RBD-R: 5'-TGCCTCGAGCTCAAGTGTCTGTGGATCAC-3'). Each quantification was performed in triplicate.

Immunofluorescence Analysis

The expression of angiotensin-converting enzyme 2 (ACE2) and the SARS-CoV-2 nucleoprotein was analyzed using immunofluorescence with the anti-SARS-CoV-2 nucleocapsid protein (NB100-56576; Novus Biologicals, Basel, Switzerland; Centennial, 1:250 dilution) and anti-ACE2 (clone EPR4435-2, 1:250 dilution; Abcam, Cambridge, MA, USA) antibodies.²⁵

Statistical Analysis

Statistical comparisons of the qRT-PCR data of the control and treatment groups were performed using the Student's *t*-test as the data displayed a normal distribution based on the Kolmogorov-Smirnov test. Differences were considered significant at $P < 0.05$. Statistical analyses were performed using GraphPad Prism version 8 (GraphPad, San Diego, CA, USA).

Results

Effects of OED on hCE-2 Cell Growth

First, we assayed the effects of different concentrations of OED on the proliferation of hCE-2 cells, an established model system for the scratch test. After 72 hours of culture, 100 to 300 μ L of OED were found to

have a negligible effect on the extent of growth (viability: $98\% \pm 2\%$), which was assayed as the viable cell number detected using the trypan blue dye exclusion test. However, 400 to 500 μ L were identified to be slightly cytotoxic (viability: $80\% \pm 5\%$) (Fig. 2a). As a result, we proceeded to assess the effect of 100 μ L of OED.

Scratch Test

The hCE-2 cells were cultured in a monolayer, and a scratch was obtained with culture-insert two-well as previously reported. As shown in Figure 2b, the OED could restore $50\% \pm 5\%$ of the scratch in the cell monolayer compared with the $25\% \pm 3\%$ obtained after PBS treatment (Fig. 2c, $P < 0.001$; Student's *t*-test).

Dry Eye Assay

The corneal tissues were tested for their ability to restore the physiological status of DED. The corneal tissues were maintained at 43°C for 24 hours to simulate a dry eye condition. Thereafter, the tissues were treated with 100 μ L/day. The corneal tissues were then harvested and used in SEM analysis, hematoxylin and eosin staining, and real-time PCR to detect the inflammatory marker (interleukin [IL]-8) and matrix metalloproteinase-9 (MMP-9).^{26,27}

Figure 3 shows the overall morphology of the control corneal tissue, control dry eye, and the dry eye treated with OED for 24 hours, as observed under a light microscope. The tissue morphology of the control was preserved (Figs. 3a–3c), with a flattened layer of non-keratinized superficial cells, an intermediate cell layer, and cells displaying lateral cytoplasmic extensions similar to wing cells. Furthermore, the basal layer of the regular column cuboidal cells was clearly visible.

A remarkable reduction in the thickness of the epithelium was observed in the dry eye condition compared with that in the control (Figs. 3d–3f). Notably, the epithelium in the corneal tissues (experimentally induced dry eye in vitro) was viable, as assessed by the expression of the housekeeping gene using qRT-PCR (Fig. 5a). The reduction in thickness appears to be related to the loss of water due to the severe dry experimental conditions. Therefore, we concluded that low humidity and high temperature could reproduce the dry environmental conditions that cause ocular discomfort and inflammation. Treatment with OED restored the basal condition, ultimately preserving the corneal cells from dehydration (Figs. 3g–3i).

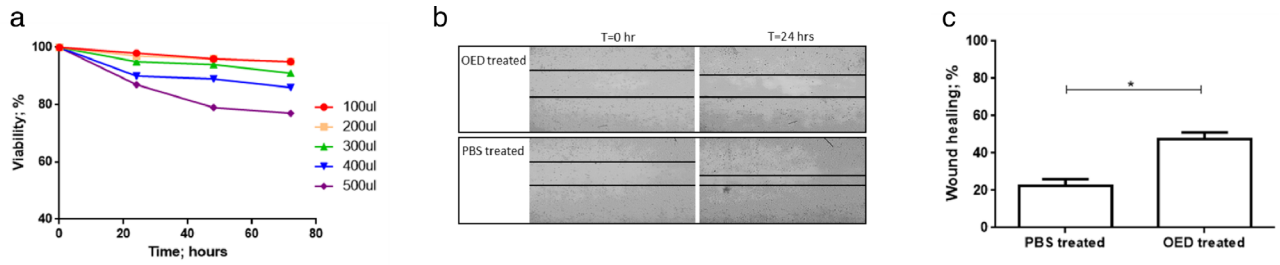


Figure 2. (a) Effect of different doses of OED on the proliferation of hCE-2 cells after 72 hours of culture. From 100 µL to 300 µL of OED/day, a negligible effect on the extent of growth was observed. However, 400 µL to 500 µL of OED/day resulted in cytotoxic effects. (b, c) Scratch assay: representative results in the hCE-2 cell line after 24 hours of treatment with OED and PBS.

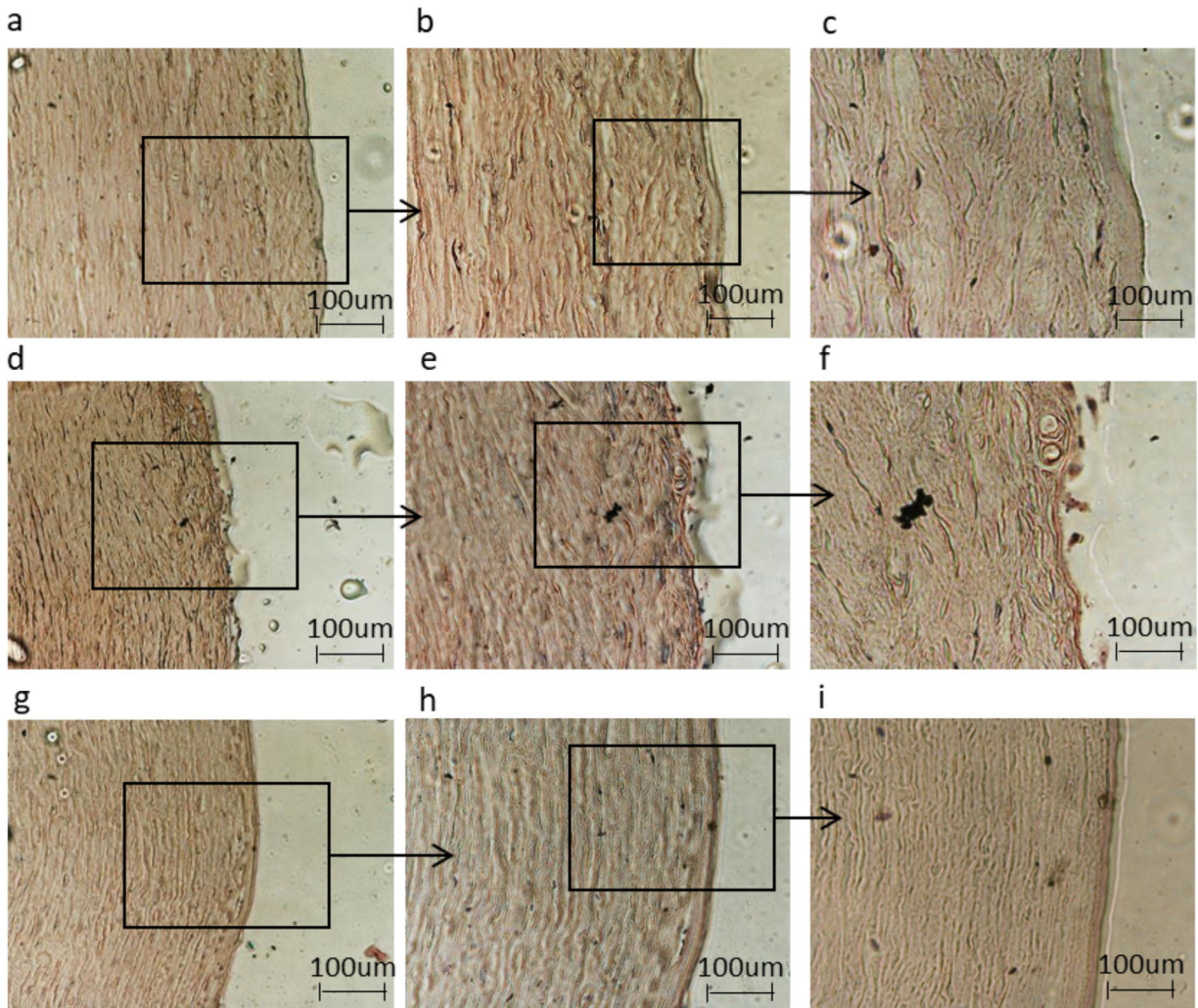


Figure 3. Histomorphological analysis of (a, b, c) control group corneal tissues, (d, e, f) control dry eye, and (f, g, h) dry eye corneal tissues treated with ozonated-oil liposome eyedrop gel. Magnifications $\times 4$, $\times 10$, and $\times 20$.

Microvilli Analysis Using SEM

SEM analysis revealed that the control tissue was rich in microvilli and mucin networks (Figs. 4a, 4b). A significant reduction in the number of microvilli

and mucin networks was observed after the induction of the dry eye condition (Figs. 4c, 4d). At 24 hours after treatment with OED, the number of microvilli and the mucin network were restored (Figs. 4e, 4f).

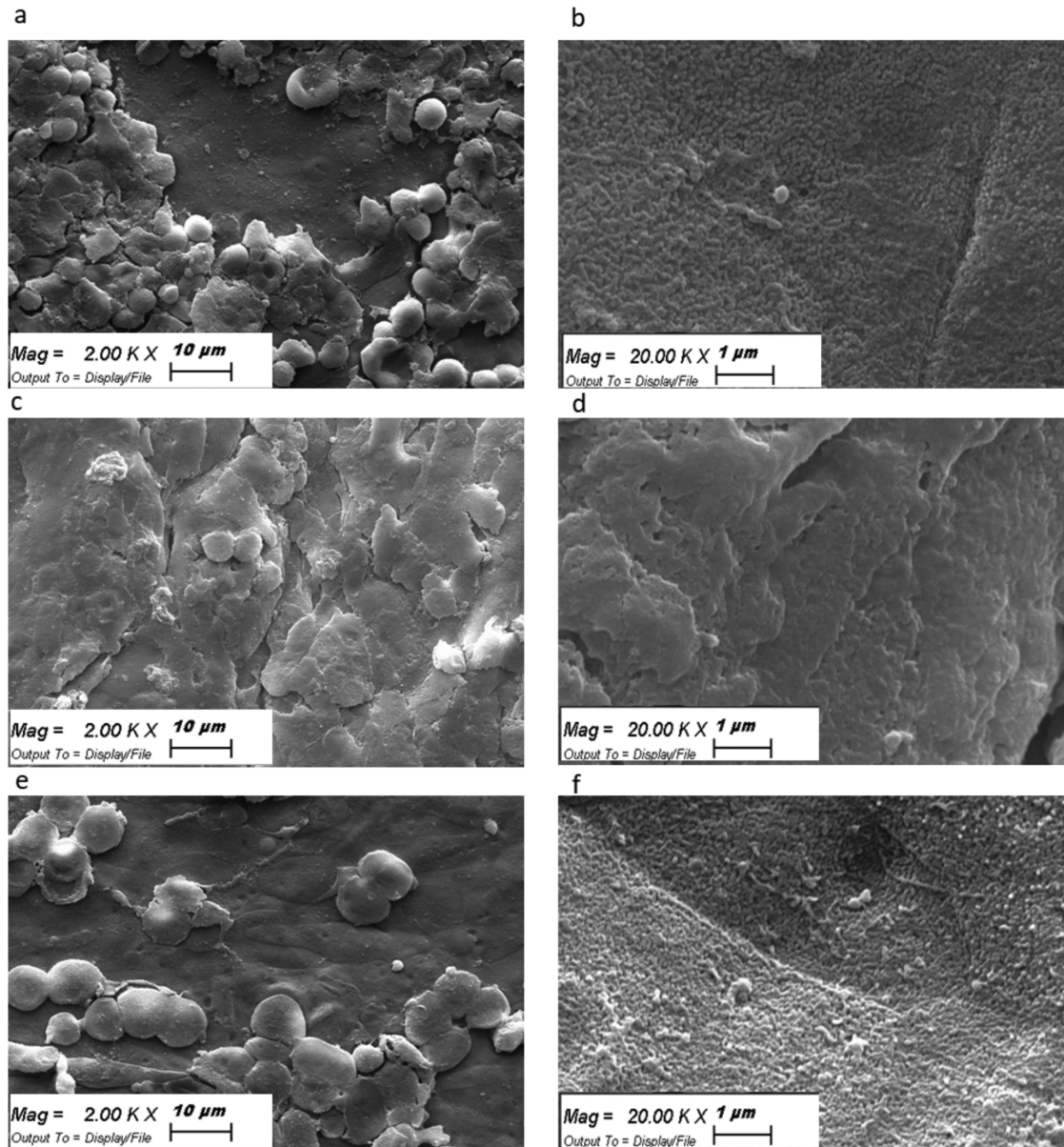


Figure 4. Scanning electron microscopy images of human corneal microvilli and mucin network in (a, b) control, (c, d) dry eye, and (e, f) OED-treated dry eye condition. Different magnifications are reported.

Quantification of MMP9 and IL-8 mRNAs

We tested duplicate corneal tissue samples in the gene expression studies. Transcriptional analysis using qRT-PCR confirmed the viability of the cells in all culture conditions. Furthermore, the housekeeping gene, *GAPDH*, was found to be equally expressed in all experimental settings (Fig. 5a). However, the expression of the inflammatory cytokine, IL-8, was increased by twofold at 24 hours after the induction of the dry eye condition ($P < 0.001$; Student's *t*-test) (Fig. 5a). Treatment with OED restored the basal levels of IL-8. Furthermore, a ninefold overexpres-

sion from the basal level of MMP-9 was observed at 24 hours after dry eye induction (Fig. 5b). However, treatment with OED restored the basal levels of MMP-9.

Effects of OED on Vero E6 Cell Growth

First, we assayed the effects of different concentrations of the OED gel on the proliferation of Vero E6 cells, an established model system for SARS-CoV-2 replication. After 72 hours of culture, 100 to 300 μ L of OED were found to have a negligible effect on the extent of growth, which was assayed as the viable

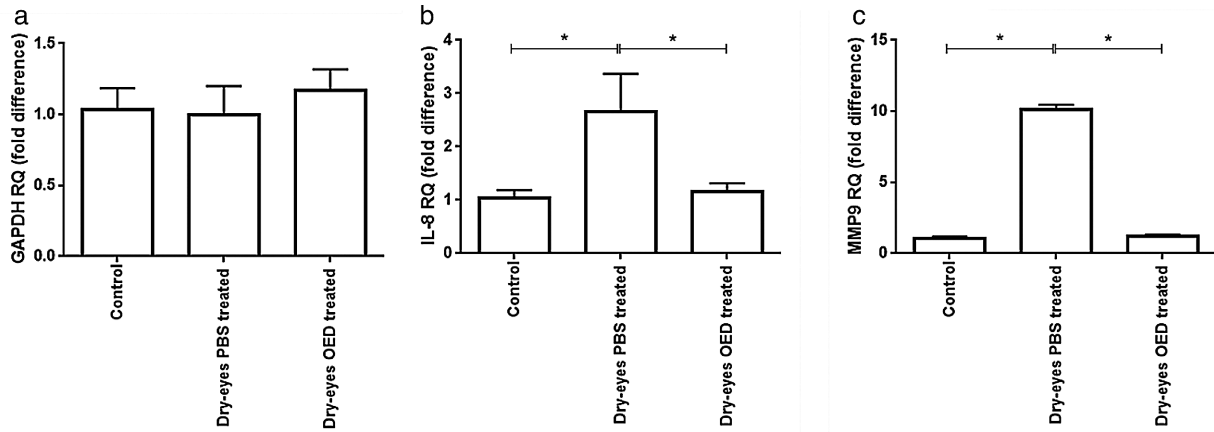


Figure 5. Quantitative reverse transcription polymerase chain reaction results of (a) *GAPDH*, (b) *IL-8*, and (c) *MMP9* levels in corneal tissues under normal conditions (37°C) and dry eye condition (Dry eyes) without (PBS-treated) or with OED treatment (OED treated). The results are expressed as the mean of triplicate experiments after 24 hours of treatment.

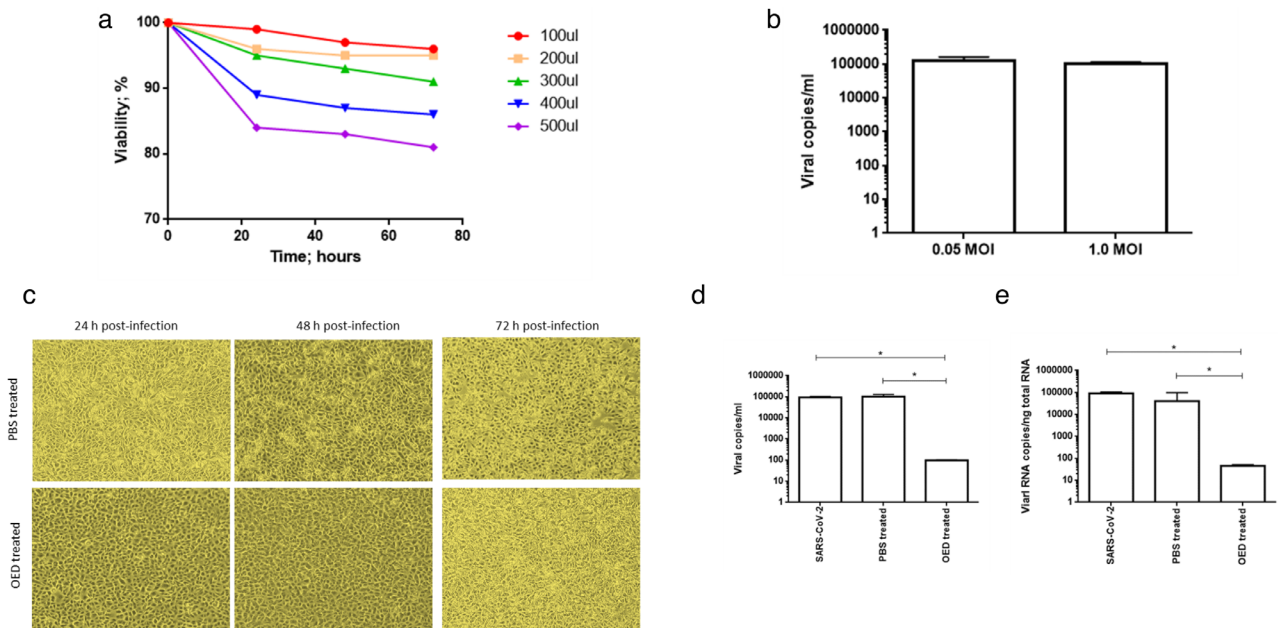


Figure 6. (a) Effect of different doses of OED on the proliferation of Vero E6 cells after 72 hours of culture. From 100 µL to 300 µL of OED/day, a negligible effect on the extent of growth was observed; however, from 400 µL to 500 µL of OED/day, a cytotoxic effect was indicated. (b) Vero E6 cells were infected with SARS-CoV-2 at a multiplicity of infection of 0.05 or 1.0 for one hour at 37°C. Thereafter, the cells were washed and cultured for 48 hours. Viral yield was quantified in the cell supernatant using quantitative reverse-transcription PCR (qRT-PCR). At least three independent replicates were tested. Data are representative of three independent experiments. Vero E6 cells were infected with SARS-CoV-2 at an MOI of 0.05 in the absence or presence of OED. (c) Images of cells were captured with an optical microscope to detect the typical SARS-CoV-2-induced cytolitic effects. (d) Viral yield was quantified in the cell supernatant using qRT-PCR. At least three independent replicates were tested. Data are representative of three independent experiments (* $P < 0.001$). (e) Quantitation of SARS-CoV-2 genome at the intracellular level using qRT-PCR. At least three independent replicates were analyzed. Data are representative of three independent experiments. (* $P < 0.001$).

cell number detected using the trypan blue dye exclusion test (viability: $94\% \pm 3\%$). However, 400 to 500 µL resulted in cytotoxicity (viability: $81\% \pm 5\%$) (Fig. 6a). As a result, we proceeded with the use of 100 µL of OED.

OED Strongly Inhibits SARS-CoV-2 Replication

Vero E6 cells were either infected at a low MOI (0.05) or high MOI (1.0). Quantification of

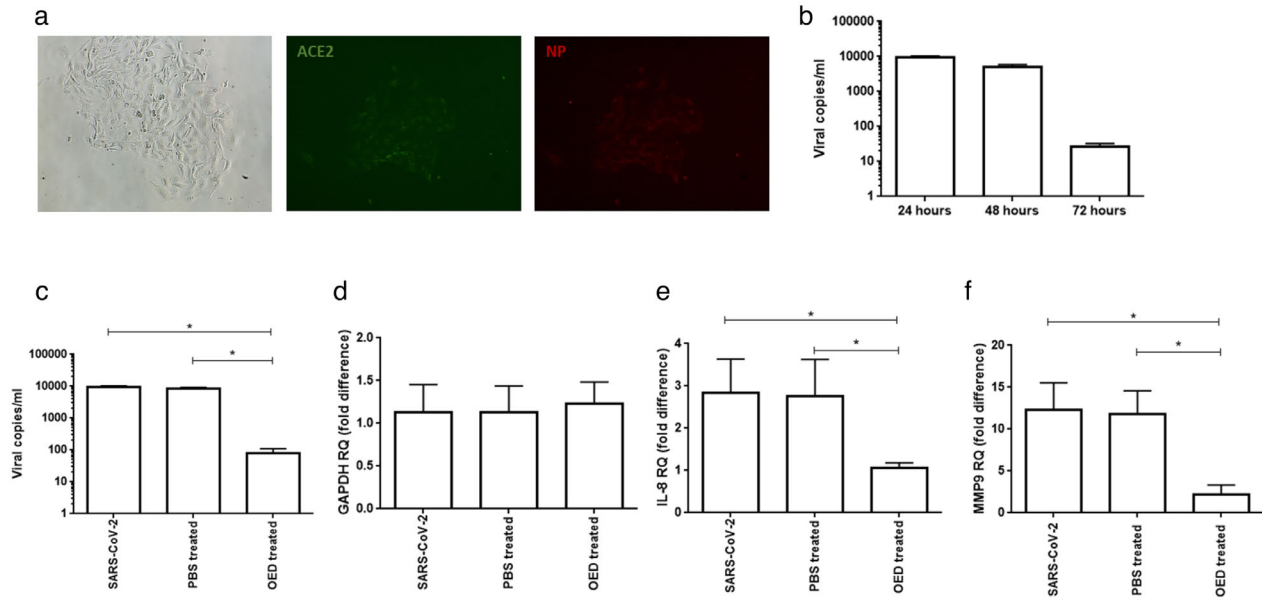


Figure 7. (a) Immunofluorescence analysis of the expression of angiotensin-converting enzyme 2 (ACE2) (*middle panel*) and the SARS-CoV-2 nucleoprotein (*right panel*) on the surfaces of hCE-2 cells infected with SARS-CoV-2 at an MOI of 1.0 for 24 hours. A Nikon Eclipse TE2000S system equipped with 621 was used as the digital camera; original magnification $\times 10$. (b) hCE-2 cells were infected with SARS-CoV-2 at an MOI of 1.0 for one hour at 37 °C. Thereafter, the cells were washed and cultured for 48 hours. Viral yield was quantified using the cell supernatant with quantitative reverse-transcription PCR (qRT-PCR). At least three independent replicates were assessed. Data are representative of three independent experiments. hCE-2 cells were infected with SARS-CoV-2 at an MOI of 1.0 in the absence or presence of OED. (c) Viral yield was quantified in the cell supernatant using qRT-PCR. At least three independent replicates were analyzed. Data are representative of three independent experiments. (* $p < 0.001$). qRT-PCR results for (d) *GAPDH*, (e) *IL-8*, and (f) *MMP9* in hCE-2 after 24 hours of infection with SARS-CoV-2 at an MOI of 1.0 without (PBS-treated) or with OED (OED-treated). The results are expressed as the mean of triplicate experiments after 24 hours of treatment (* $P < 0.001$).

the released RNA after 48 hours indicated that viral production ($100,000 \pm 1200$ copies/mL) was very similar at both MOIs (Fig. 6b). Therefore, in the subsequent experiments, an MOI of 0.05 was used.

We proceeded to determine whether OED could affect the replication of SARS-CoV-2. Briefly, Vero E6 cells were infected with a primary SARS-CoV-2 strain isolated in Brescia, Italy. After one hour, the cells were cultured in the absence or presence of OED, with 100 μ L administered every 10 hours, as recommended for the product. OED efficiently inhibited viral replication (Fig. 6c). In fact, OED abolished the SARS-CoV-2 cytolitic effects on Vero E6 cells, with only limited detectable cytopathic effects observed at 72 hours after infection; this finding may be due to cell senescence (Fig. 6c). Quantification of viral RNA copy number in the cell culture supernatants confirmed the potent inhibitory effect of OED on viral particle production, with a reduction of nearly four logarithms at 72 hours after infection relative to that observed in untreated and PBS-treated infected cells (Fig. 6d). The qRT-PCR quantification of intracellular SARS-CoV-2 RNA in SARS-CoV-2-infected cells confirmed the inhibition

of almost four logarithms of the intracellular SARS-CoV-2 genome expression in the presence of OED compared with that in the untreated and PBS-treated cells (Fig. 6e).

SARS-CoV-2 Replication was Not Assessed in hCE-2 Cells

To determine whether OED interfered with SARS-CoV-2 replication in corneal cells, we infected hCE-2 cells with the virus. Furthermore, to confirm that hCE-2 cells presented the main SARS-CoV-2 receptor, ACE2, we performed an immunofluorescence assay. A slight expression of ACE2 was observed in hCE-2 cells (Fig. 7a), supporting the possibility of SARS-CoV-2 infection. However, quantification of the released RNA after 24, 48, and 72 hours of infection indicated that viral production was very low in hCE-2 cells (Fig. 7b). The highest SARS-CoV-2 RNA expression was observed at 24 hours, as revealed using immunofluorescence analysis, with a slight expression of the viral nucleoprotein (Fig. 7a). These results suggest the

ability of SARS-CoV-2 to infect corneal cells, that are able to sustain a 48-hour viral replication (Fig. 7b). We proceeded to determine the possible efficacy of OED on corneal cells within the 24 hours after infection. In the presence of OED, SARS-CoV-2 RNA expression was found to decrease at 24 hours after infection compared with that observed in untreated cells or cells treated with PBS. The low SARS-CoV-2 replication in hCE-2 cells was counterbalanced by the expression of inflammatory molecules. By assessing the expression levels of IL-8 and MMP9, we found that during the first 24 hours of infection, an increased expression of IL-8 and MMP9 occurred in hCE-2 cells which was restored to basal level in the presence of OED (Figs. 7e, 7f).

Discussion

The effects of SARS-CoV-2 are becoming increasingly well known and are causing the global population to panic. No one seems to be spared from this virus, and the predisposing factors for a more aggressive infection are still unknown. As we await a vaccine that can reduce the spread of the virus, there are few defenses that can be deployed to reduce the risk of contagion.

The role of the ocular surface as a possible portal of entry, reservoir for replication, and site of transmission of SARS-CoV-2 RNA has been explored extensively.^{28–30} Recently, live virus has been identified in ocular fluids based on the cytopathic effects observed in Vero E6 cells.³¹ Both corneal and conjunctival epithelia express ACE2, DC-SIGN/DC-SIGNR, and TMPRSS2, suggesting that the ocular surface is a potential route for the transmission of SARS-CoV-2.³² Because contagion through the eye can occur, strategies to reduce the risk of virus entry should be evaluated. The ocular contagion risk increases in cases of tear film abnormalities, such as in DED. In these cases, the epithelial conjunctival microvilli have incipient epithelial damage, and the ocular surface is more vulnerable to infectious microorganisms.³³

Although new molecules are being explored for their potential defensive effects against SARS-CoV-2, we opted to focus on O₃. Ozone-mediated virus inactivation occurs primarily in two ways: lipid peroxidation and protein peroxidation. Herein, OED was found to efficiently inhibit viral replication at the post-entry stages of SARS-CoV-2 infection. The *in vitro* administration of OED was able to reduce the SARS-CoV-2 infection relative to that observed in the untreated state. Topical OED administration might reduce the risk of SARS-CoV-2 infection through the ocular surface and could be an essential safeguarding procedure not

only for healthcare professionals but also for the entire population. The main limitation of this study is the absence of *in vivo* confirmation in an animal model that has to be performed before clinical application.

The OED gel efficiently restored cell regeneration and controlled cell inflammation during the dry eye condition. Furthermore, the presence of the ACE2 receptors and TMPRSS2 protein on the corneal limbal stem cells may theoretically allow the beta coronavirus to cross the ocular surface and subsequently spread from the eye to other parts of the body through the blood stream or the nervous system (ophthalmic branch of trigeminal nerve).³⁴ Although there is no current evidence to suggest that the SARS-CoV-2 virus, in humans, can enter the eye or spread to the brain through the corneal nerves, in some animal models (feline and murine), beta coronaviruses caused several ocular infections (e.g., conjunctivitis, uveitis, retinitis, and optic neuritis), thereby suggesting that they could penetrate the ocular globe in some mammals.³⁵

The anti-inflammatory potential of OED might be important in the control of SARS-CoV-2 inflammation, which is reported to be the basis of viral pathogenicity. SARS-CoV-2 conjunctivitis has been described as a mild follicular conjunctivitis, otherwise indistinguishable from other viral threats, that can be transmitted via aerosol contact with the conjunctiva.³⁶ These literature data and the expression of viral entry factors (ACE2, TMPRSS2) suggest that also conjunctival epithelium, which covers a much larger area of the ocular surface, might be evaluated for its role in SARS-CoV-2 infection through ocular transmission.

Other features of ocular surface involvement include unilateral or bilateral bulbar conjunctiva hyperemia alone or in association with chemosis, follicular reaction of the palpebral conjunctiva, watery discharge, epiphora, and mild eyelid edema. The prevalence of conjunctivitis in patients with COVID-19 remains controversial. Although only 0.9% of patients were found to develop signs of conjunctivitis,³⁷ another report indicated that up to 31.6% of hospitalized patients had conjunctivitis.³⁸ However, in the latter study, only about 5% of patients with positive findings for COVID-19 based on RT-PCR using nasopharyngeal swabs had a positive conjunctival swab. Moreover, only one of the 38 patients displayed conjunctivitis as their first symptom. Patients with ocular symptoms are more likely to have higher white blood cell and neutrophil counts, as well as higher levels of procalcitonin, C-reactive protein, and lactate dehydrogenase than patients without ocular symptoms. In one patient, the RT-PCR assay revealed the presence of viral RNA in the conjunctival specimen 13 days after disease onset. Furthermore, the conjunctival swab

specimens remained positive for SARS-CoV-2 at days 14 and 17 following onset. However, on day 19, the RT-PCR result was negative for SARS-CoV-2.²⁶ In another report, one hospitalized patient had SARS-CoV-2-positive conjunctival swabs up to day 21 from symptom onset; however, after a few days, the virus was undetectable in nasal swabs. Five days later, the virus was undetectable in the conjunctival swab but was detected on day 27, suggesting sustained replication of the virus in the conjunctiva.³¹

Although the acquiring of SARS-CoV-2 infection through ocular transmission is remarkably concerning, its underlying mechanism has not been clarified.²⁸ We can hypothesize that SARS-CoV-2 is transported from the infected ocular surface to the respiratory and digestive tract through the lacrimal canaliculi (which drains tears from the eye surface into the nasal cavity), regardless of a more or less significant presence of the ACE2 receptors on the cornea and conjunctiva.^{39,40} Altogether, dry eye condition might be a risk factor for SARS-CoV-2 infection and the use of OED might have a preventive role. In the future, we will test the effects of OED in vivo to better understand its preventive role.

Acknowledgments

The authors thank Iva Pivanti and Mercedes Fernandez for providing technical support and Paola Boldrini for performing the electron microscopy analysis.

Supported by the University of Ferrara FAR, COVID19 Unife Grant and University of Ferrara Crowdfunding program.

Disclosure: **S. Rizzo**, None; **M.C. Savastano**, None; **D. Bortolotti**, None; **A. Savastano**, None; **G. Gambini**, None; **F. Caccuri**, None; **V. Gentili**, None; **R. Rizzo**, None

* SR and MCS contributed equally in the drafting of the manuscript.

‡ VG and RR contributed equally in the planning the research.

References

- Lu CW, Liu X, Jia ZF. 2019-nCoV transmission through the ocular surface must not be ignored. *Lancet*. 2020;e39:395.
- Chen L, Liu M, Zhang Z, et al. Ocular manifestations of a hospitalised patient with confirmed 2019 novel coronavirus disease. *Br J Ophthalmol*. 2020;104:748–751.
- Xia J, Tong J, Liu M, Shen Y, Guo D. Evaluation of coronavirus in tears and conjunctival secretions of patients with SARS-CoV-2 infection. *J Med Virol*. 2020;92:589–594.
- Bozkurt E, Özateş S, Muhafız E, et al. Ocular surface and conjunctival cytology findings in patients with confirmed COVID-19. *Eye Contact Lens Sci Clin Pract*. 2021;47(4):168–173.
- Valente P, Iarossi G, Federici M, et al. Ocular manifestations and viral shedding in tears of pediatric patients with coronavirus disease 2019: a preliminary report. *J Am Assoc Pediatr Ophthalmol Strabismus*. 2020;24:212–215.
- Coroneo MT. The eye as the discrete but defensible portal of coronavirus infection. *Ocul Surf*. 2021;19:176–182.
- Yang J, Petitjean SJL, Koehler M, et al. Molecular interaction and inhibition of SARS-CoV-2 binding to the ACE2 receptor. *Nat Commun*. 2020;11:4541.
- Araimo F, Imperiale C, Tordiglione P, et al. Ozone as adjuvant support in the treatment of COVID-19: a preliminary report of probiozovid trial. *J Med Virol*. 2020;93:2210–2220
- Elvis AM, Ekta JS. Ozone therapy: a clinical review. *J Nat Sci Biol Med*. 2011;2(1):66–70.
- Cattel F, Giordano S, Bertiond C, et al. Ozone therapy in COVID-19: a narrative review. *Virus Res*. 2021;291:198207.
- Kim HS, Noh SU, Han YW, et al. Therapeutic effects of topical application of ozone on acute cutaneous wound healing. *J Korean Med Sci*. 2009;24:368–374.
- Celenza G, Iorio R, Cracchiolo S, et al. Antimycotic activity of ozonized oil in liposome eye drops against *Candida spp*. *Transl Vis Sci Technol*. 2020;9(8):4.
- Bocci V, Larini A, Micheli V. Restoration of normoxia by ozone therapy may control neoplastic growth: a review and a working hypothesis. *J Altern Complement Med*. 2005;11:257–265.
- Valacchi G, Fortino V, Bocci V. The dual action of ozone on the skin. *Br J Dermatol*. 2005;153:1096–1100.
- Sechi LA, Lezcano I, Nunez N, et al. Antibacterial activity of ozonized sunflower oil (Oleozone). *J Appl Microbiol*. 2001;90:279–284.
- Ugazio E, Tullio V, Binello A, et al. Ozonated oils as antimicrobial systems in topical applications. their characterization, current applications,

- and advances in improved delivery techniques. *Molecules*. 2020;25:334.
17. Spadea L, Tonti E, Spaterna A, Marchegiani A. Use of ozone-based eye drops: a series of cases in veterinary and human spontaneous ocular pathologies. *Case Rep Ophthalmol*. 2018;9:287–298.
 18. Marchegiani A, Magagnini M, Cerquetella M, et al. Preoperative topical liposomal ozone dispersion to reduce bacterial colonization in conjunctival sac and periocular skin: Preliminary study in dogs. *Exp Eye Res*. 2019;189:107848.
 19. Mazzotta C, Giancipoli E. Anterior acute uveitis report in a SARS-CoV-2 patient managed with adjunctive topical antiseptic prophylaxis preventing 2019-nCoV spread through the ocular surface route. *Int Med Case Rep J*. 2020;13:513–520.
 20. JÁP Gomes, JAP Milhomens Filho. Iatrogenic corneal diseases or conditions. *Exp Eye Res*. 2021;203:108376.
 21. Schrage NF, Flick S, von Fischern T, Reim M, Wenzel M. Temperature changes of the cornea by applying an eye bandage. *Ophthalmologe*. 1997;94:492–495.
 22. de Wilde AH, Raj VS, Oudshoorn D, et al. MERS-coronavirus replication induces severe in vitro cytopathology and is strongly inhibited by cyclosporin A or interferon- α treatment. *J Gen Virol*. 2013;94(Pt 8):1749–1760.
 23. Caruso A, Caccuri F, Bugatti A, et al. Methotrexate inhibits SARS-CoV-2 virus replication “in vitro.” *J Med Virol*. 2020;93:1780–1785.
 24. Caccuri F, Zani A, Messali S, et al. A persistently replicating SARS-CoV-2 variant derived from an asymptomatic individual. *J Transl Med*. 2020;18:362.
 25. Rizzo R, Neri LM, Simioni C, et al. SARS-CoV-2 nucleocapsid protein and ultrastructural modifications in small bowel of a 4-week-negative COVID-19 patient. *Clin Microbiol Infect*. 2021;27:936–937.
 26. Wu X, Chen X, Ma Y, et al. Analysis of tear inflammatory molecules and clinical correlations in evaporative dry eye disease caused by meibomian gland dysfunction. *Int Ophthalmol*. 2020;40:3049–3058.
 27. Chotikavanich S, de Paiva CS, Li DQ, et al. Production and activity of matrix metalloproteinase-9 on the ocular surface increase in dysfunctional tear syndrome. *Invest Ophthalmol Vis Sci*. 2009;50:3203–3209.
 28. Sadhu S, Agrawal R, Pyare R, et al. COVID-19: limiting the risks for eye care professionals. *Ocul Immunol Inflamm*. 2020;28:714–720.
 29. Zou L, Ruan F, Huang M, et al. SARS-CoV-2 viral load in upper respiratory specimens of infected patients. *N Engl J Med*. 2020;382:1177–1179.
 30. Lu C-W, Liu X-F, Jia Z-F. 2019-nCoV transmission through the ocular surface must not be ignored. *Lancet*. 2020;395(10224):e39.
 31. Colavita F, Lapa D, Carletti F, et al. SARS-CoV-2 isolation from ocular secretions of a patient with COVID-19 in Italy with prolonged viral RNA detection. *Ann Intern Med*. 2020;173:242–243.
 32. Roehrich H, Ching Y, Hou JH. Immunohistochemical study of SARS-CoV-2 viral entry factors in the cornea and ocular surface. *Cornea*. 2020;39:1556–1562.
 33. Cennamo GL, Del Prete A, Forte R, et al. Impression cytology with scanning electron microscopy: a new method in the study of conjunctival microvilli. *Eye (Lond)*. 2008;22:138–143.
 34. Li Y-C, Bai W-Z, Hashikawa T. The neuroinvasive potential of SARS-CoV2 may play a role in the respiratory failure of COVID-19 patients. *J Med Virol*. 2020;92:552–555.
 35. Seah I, Agrawal R. Can the coronavirus disease 2019 (COVID-19) affect the eyes? A review of coronaviruses and ocular implications in humans and animals. *Ocul Immunol Inflamm*. 2020;28:391–395.
 36. Chen L, Liu M, Zhang Z, et al. Ocular manifestations of a hospitalised patient with confirmed 2019 novel coronavirus disease. *Br J Ophthalmol*. 2020;104:748–751.
 37. Guan W-J, Ni Z-Y, Hu Y, et al. Clinical characteristics of coronavirus disease 2019 in China. *N Engl J Med*. 2020;382:1708–1720.
 38. Wu P, Duan F, Luo C, et al. Characteristics of ocular findings of patients with coronavirus disease 2019 (COVID-19) in Hubei Province, China. *JAMA Ophthalmol*. 2020;138:575–578.
 39. Sun Y, Liu L, Pan X, Jing M. Mechanism of the action between the SARS-CoV S240 protein and the ACE2 receptor in eyes. *Int J Ophthalmol*. 2006;6:783–786.
 40. Sun K, Gu L, Ma L, Duan Y. Atlas of ACE2 gene expression reveals novel insights into transmission of SARS-CoV-2. *Heliyon*. 2021;7(1):e05850.